STEM CELLS AND DEVELOPMENT
Volume 22, Number 19, 2013

DOI: 10.1089/scd.2012.0714

ARS-Interacting Multi-Functional Protein 1 Induces Proliferation of Human Bone Marrow-Derived Mesenchymal Stem Cells by Accumulation of β-Catenin via Fibroblast Growth Factor Receptor 2-Mediated Activation of Akt

Seo Yoon Kim,[1,*] Woo Sung Son,[2,*] Min Chul Park,[3] Chul Min Kim,[1] Byung Hyun Cha,[1] Kang Jun Yoon,[4] Soo-Hong Lee,[1] and Sang Gyu Park[1,5]

ARS-Interacting Multi-functional Protein 1 (AIMP1) is a cytokine that is involved in the regulation of angiogenesis, immune activation, and fibroblast proliferation. In this study, fibroblast growth factor receptor 2 (FGFR2) was isolated as a binding partner of AIMP peptide (amino acids 6–46) in affinity purification using human bone marrow-derived mesenchymal stem cells (BMMSCs). AIMP1 peptide induced the proliferation of adult BMMSCs by activating Akt, inhibiting glycogen synthase kinase-3β, and thereby increasing the level of β-catenin. In addition, AIMP1 peptide induced the translocation of β-catenin to the nucleus and increased the transcription of c-myc and cyclin D1 by activating the β-catenin/T-cell factor (TCF) complex. By contrast, transfection of dominant negative TCF abolished the effect of AIMP1. The inhibition of Akt, using LY294002, abolished the accumulation and nuclear translocation of β-catenin induced by AIMP1, leading to a decrease in c-myc and cyclin D1 expression, which decreased the proliferation of BMMSCs. An intraperitoneal injection of AIMP1 peptide into C57/BL6 mice increased the colony formation of fibroblast-like cells. Fluorescence activated cell sorting analysis showed that the colony-forming cells were $CD29^+/CD44^+/CD90^+/CD105^+/CD34^-/CD45^-$, which is characteristic of MSCs. In addition, the fibroblast-like cells differentiated into adipocytes, chondrocytes, and osteocytes. Taken together, these data suggest that AIMP1 peptide promotes the proliferation of BMMSCs by activating the β-catenin/TCF complex via FGFR2-mediated activation of Akt, which leads to an increase in MSCs in peripheral blood.

Introduction

Mesenchymal stem cells (MSCs) are isolated as fibroblast-like cells in bone marrow (BM) colonies; they are nonhematopoietic stromal multipotent stem cells that can differentiate into multiple types of cells such as adipocytes, chondrocytes, and osteocytes, under appropriate conditions [1–8]. In addition, MSCs have been isolated from the fetal liver, umbilical cord blood, BM, and adipose tissue [9–11]. They are characterized by the expression of surface markers such as CD105, CD73, and CD90 [12]. The multipotency of MSCs makes them an attractive potential source of cells for cell therapy in regenerative medicine [13]. Furthermore, since MSCs can be directly obtained from individual patients, the complications associated with the immune rejection of allogenic tissue can be avoided. Since the homing efficiency of MSCs to target sites is low, large numbers of MSCs are required for the efficient regeneration of damaged tissue. However, since there are limitations to obtaining sufficient amounts of MSCs from a single patient, in vitro expansion that preserves their differentiation and proliferative potential is needed. Currently, in vitro expansion to apply to clinical therapy has limitations due to the animal factor of culture media. Thus, culture media containing a variety of growth factors instead of serum has been developed. In addition, the development of new agents that can induce the proliferation of MSCs without affecting their differentiation potential is required. Recently, many studies have reported that sphingosine-1-phosphate (S1P) and growth factors, including epidermal growth factor (EGF) and fibroblast growth factor

[1]Laboratory for Tracing of Gene Function, Department of Biomedical Science, CHA University, Sungnam-si, Korea.
[2]Department of Pharmacy, College of Pharmacy, CHA University, Pocheon-si, Korea.
[3]Medicinal Bioconvergence Research Center, Seoul National University, Seoul, Korea.
[4]Department of Neurosurgery, St. Peter's Kangnam Hospital, Seoul, Korea.
[5]CHA Stem Cell Institute, Seoul, Korea.
*These authors contributed equally to this work.

(FGF), induce the proliferation of MSCs without affecting multipotency [14–17].

ARS-interacting multifunctional protein 1(AIMP1) was originally identified as a member of the mammalian multi-ARS complex [18]. AIMP1 is secreted in response to hypoxia and cytokine stimulation; it functions as a cytokine with various target cells including endothelial cells, monocyte/macrophage cells, dendritic cells, and pancreatic α cells [19–26]. Recently, macrophages were shown to secrete on stimulation with tumor necrosis factor α in wound lesions, and AIMP1 was shown to enhance wound healing, which was mediated by fibroblast proliferation and collagen synthesis via ERK activation [20]. Deletion mapping analysis showed that the N-terminal domain (amino acids 6–46) of AIMP1 was responsible for the stimulation of fibroblast proliferation [27]. Since the proliferation of MSCs is critical to providing a reservoir of cells or back up for the repair or regeneration of damaged tissues, we studied AIMP1 to determine whether it could promote the proliferation of BMMSCs. The results of this study showed that AIMP1 peptide increased the expression of cyclin D1 and c-myc by stabilizing β-catenin via FGF receptor 2 (FGFR2)-mediated activation of Akt. This promoted the proliferation of BMMSCs without affecting their differentiation into adipocytes, chondrocytes, and osteocytes.

Materials and Methods

Cell culture and proliferation assay

BMMSCs were purchased from PromoCell and were maintained in low-glucose Dulbecco's modified Eagle's medium (DMEM) supplemented with 10% fetal bovine serum (FBS) and 1% streptomycin/penicillin. Cells between passages 4 and 7 were used for this study. For the 3-(4,5-dimethylthiazol-2-yl)-2,5-diphenyltetrazolium bromide (MTT) assay, human BMMSCs (1×10^4 cells) were seeded onto 96-well plates and cultured for 24 h. After serum starvation for 4 h with low-glucose DMEM containing 0.5% FBS, the BMMSCs were treated with different concentrations of AIMP1 peptide (amino acids 6–46) in the presence or absence of LY294002 (10 μM) (Calbiochem) and U0126 (10 μM)(Calbiochem). BmMSCs were cultured for 24 h. Subsequently, 10 μL of Ez-Cytox (DaeilLab) was added to each well, and the cells were cultured for another 4 h. At the end of the incubation, we evaluated cell viability by measuring the optical density at 450 nm. For the cell counting assay, human BMMSCs (1.2×10^4 cells) were seeded onto 24-well plates and cultured in low-glucose DMEM supplemented with 10% FBS and 1% streptomycin/penicillin for 12 h. After serum starvation for 4 h with low-glucose DMEM containing 0.5% FBS, human BMMSCs were treated with different concentrations of AIMP1 peptide for the indicated time. The cells were stained with tryphan blue and counted using a hemacytometer under a light microscope.

Immunoblot

Human BMMSCs (2×10^5 cells) were seeded onto six-well plates and cultured for 12 h. After serum starvation for 4 h with low-glucose DMEM containing 0.5% FBS, the BMMSCs were treated with AIMP1 peptide (100 ng/mL) for the indicated time. Protein extracts of human BMMSCs were prepared with lysis buffer (20 mM HEPES, pH 7.5, 150 mM NaCl, 10% glycerol, 1% Triton X-100, 0.1% sodium dodecyl sulfate (SDS), 0.5% sodium deoxycholate, 1 mM EDTA, 10 mM sodium fluoride, 10 mM β-glycerophosphate, 0.5 mM sodium orthovanadate, and 1 mM phenylmethylsulfonyl fluoride). Forty micrograms of protein extract per lane was subjected to electrophoresis, transferred to a polyvinyldene fluoride membrane (Millipore), and blotted with their specific antibodies. Antibodies against p-glycogen synthase kinase-3β (GSK3β), GSK3β, pAkt, Akt, pERK, and ERK were purchased from Cell Signaling Technology. Antibodies against β-catenin, c-myc, HSP90, YY1, and cyclin D1 were purchased from Santa Cruz Biotechnology. Anti-tubulin antibody was purchased from Sigma-Aldrich. Antibody against FGFR2 was purchased from Abcam. To separate the nucleus and the cytoplasm, cells were lysed with hypotonic solution (10 mM HEPES, pH 7.4, 10 mM KCl, 0.5 NP40, 1.5 mM $MgCl_2$, 0.5 mM EGTA, 12 mM β-glycerophosphate, 10 mM NaF, 1 mM Na_3VO_4, 1 mM phenylmethane sulfonylfluoride (PMSF), and 5 μg/mL aprotinin) to obtain the cytoplasmic proteins. The nucleus was then lysed with 10 mM HEPES, pH 7.4, 0.3 M KCl, 1.5 mM $MgCl_2$, 0.2 mM EDTA, 12 mM β-glycerophosphate, 10 mM NaF, 1 mM Na_3VO_4, 1 mM PMSF, and 5 μg/mL aprotinin.

Immunofluorescence staining

Human BMMSCs (5×10^4 cells) were seeded onto a cover slip (9×9 mm) and cultured for 12 h. After serum starvation for 6 h with low-glucose DMEM containing 0.5% FBS, the BMMSCs were treated with AIMP1 peptide (100 ng/mL) for 2 h. The cells were fixed with 4% paraformaldehyde at room temperature (R.T) for 10 min and washed thrice with 1X phosphate-buffered saline (PBS). The cells were permeabilized with 0.1% Triton X-100 at R.T for 5 min and washed thrice with 1X PBS. The cells were blocked with 1X PBS containing 2% bovine serum albumin (BSA) at R.T for 1 h and incubated with anti-β-catenin antibody diluted 1:100 at R.T for 2 h. Thereafter, the cells were washed thrice with 1X PBS and then reacted with Alexa Fluor-488-conjugated secondary antibody (Invitrogen) at R.T for 1 h. The cell nuclei were counterstained with 4′-6′ diamidino-2-phenylindole (Invitrogen).

Luciferase assay

BMMSCs (3×10^4 cells) were seeded onto a 12-well plate and cultured in low-glucose DMEM supplemented with 10% FBS and 1% streptomycin/penicillin for 24 h. BMMSCs were then transfected with TOPflash plasmid and *Renilla* luciferase vector using Lipofectamine 2000 (Invitrogen) for 12 h. After serum starvation for 12 h with low-glucose DMEM containing 0.5% FBS, the cells were treated with AIMP1 peptide (100 ng/mL) in the presence or absence of LY294002 and U0126 for 24 h. To assess the dominant negative (DN) effect of T-cell factor (TCF), 0.1, 0.2, and 0.5 μg of TOPflash plasmid expressing DN-TCF (kindly provided by Barry M. Gumbiner, University of Virginia) was transfected into BMMSCs with the TOPflash plasmid and the *Renilla* luciferase vector and expressed for 12 h. The transfected cells were treated with AIMP1 peptide (100 ng/mL) for 24 h. Luciferase activity was measured with the Dual-Luciferase

Table 1. Primers Used for qRT-PCR

Primers	*Sequences*	*Species*
c-myc	F: 5′-CTCCTGGCAAAAGGTCAGAG-3′ R: 5′-GGCCTT TTCATTGTTTTCCA-3′	human
Cyclin D1	F: 5′-TGGTGAACAAGCTCAAGTGG-3′ R: 5′-TCCTCCTCTTCCTCCTCCTC-3′	
β-catenin	F: 5′-GACTTGGTTGGTAGGGT GGG-3′ R: 5′- GCTTGGTTAGTGTGTCAGGC-3′	
GAPDH	F: 5′-CGAGATCCCTCCAAAATCAA-3′ R: 5′-TGTGGTCATGAGTCCTTCCA-3′	
PPARγ	F: 5′-TCGCTGATGCACTG CCTATG-3′ R: 5′-GAGAGGTCCACAGAGCTGA TT-3′	Mouse
Aggrecan	F: 5′-GTGGAGCCGTGTTTCCAAG-3′ R: 5′-AGATGCTGTTGACTCGAA CCT-3′	
Osteocalcin	F: 5′-CGCTACCTTG GAGCTTCAGT-3′ R: 5′-GTTTGGCTTTAGGGCAGCAC-3′	
GAPDH	F: 5′-ACCCCAGCAAGGACACTGA GCAAG-3′ R: 5′-GGCTCCCTAGGCCCCTCC TGTTATT-3′	

Reporter Assay System (Promega) according to the manufacturer's instructions.

RT-polymerase chain reaction

Human BMMSCs (3×10^5 cells) were seeded onto a six-well plate and cultured in low-glucose DMEM containing 10% FBS and 1% streptomycin/penicillin for 12 h. After serum starvation for 4 h with low-glucose DMEM containing 0.5% FBS and 1% streptomycin/penicillin, the cells were treated with AIMP1 peptide (100 ng/mL) in the presence or absence of LY294002 and U0126 for 8 h. Total RNA was extracted using Easy-spin (iNtRON Biotechnology) according to the manufacturer's instructions. cDNA was synthesized by reverse transcription with 0.5 μg of total RNA, and each gene transcript was then amplified by quantitative reverse transcription-polymerase chain reaction (PCR) with specific primers. The primer sequences are summarized in Table 1.

Colony formation assay

C57/BL6 (male) mice were purchased from Orient Bio at 6 weeks of age and maintained until 7 weeks of age. The CHA Animal Care and Use Committee approved all animal studies (IACUC110013), and the investigation conformed to the Guide for the Care and Use of Laboratory Animals, published by the United States National Institutes of Health. AIMP1 peptide was diluted in sterile PBS and intraperitoneally injected as indicated. Mice were euthanized with isoflurane (Hana Pharm), and blood was harvested. Mononuclear cells were harvested using a Ficoll–Paque cushion (GE Healthcare). Mononuclear cells (5×10^6/well) were seeded into 0.1% gelatin-coated 12-well plates in DMEM with 10% FBS and 1% penicillin/streptomycin and maintained in a humidified chamber of 5% CO_2. Non-adherent cells were removed, and the medium was replaced every 3 days.

Flow cytometry

For the phenotypic analysis of fibroblast-like cells after passage 3, cells were resuspended in PBS containing 2% BSA and fixed with 2% paraform–aldehyde for 10 min. The cells were washed with PBS containing 2% BSA and incubated for 1 h at 4°C with the following antibodies: CD34-FITC (BD Biosciences), CD45-adenomatous polyposis coli (APC) (Miltenyi Biotec), CD105-APC (R&D Systems), CD44-APC (BD Biosciences), CD29-FITC (AbD Serotec), and CD90-APC (BioLegend). After washing twice with PBS containing 2% BSA, the cells were analyzed by flowcytometry using an FACScalibur flow cytometer (BD Immunocytometry Systems).

Differentiation of MSCs

Adipogenic differentiation was induced at a cell density of 1×10^4 cells/cm^2 in adipogenic medium (StemPro® Adipogenesis Differentiation Kit, Gibco BRL) for 14 days. Differentiated MSCs were fixed with 10% formaldehyde for 15 min at R.T, and washed once with 60% isopropanol. Cells were then stained with 0.6% (w/v) oil red O solution for 45 min and washed repeatedly with 60% isopropanol. Cells were washed twice with distilled water and examined under a light microscope. For osteogenic inductions, cells were cultured at 1×10^4 cells/cm^2 in DMEM containing 10% FBS, 1% GlutaMax (Gibco BRL), 0.2 mM ascorbic acid, 10 mM glycerol 2-phosphate (Sigma), 1% antibiotics, and 0.1 μM dexamethasone for 21 days. The differentiated osteogenic cells were fixed with 10% formaldehyde for 15 min and washed thrice with deionized water. Cells were then incubated in 5% silver nitrate and exposed to strong light for 1 h. The reaction was stopped by treatment with sodium thiosulfate, and cells were examined under a light microscope. To induce chondrogenic differentiation, cells were cultured at 1×10^4 cells/cm^2 for 21 days in DMEM containing 10% FBS, 1% antibiotics, 1% Insulin-Transferrin-Selenium-A Supplement (Gibco BRL), 50 μM ascorbic acid, 100 nM dexamethasone (Sigma), and 10 ng/mL transforming growth factor-beta 1 (ProSpecTany TechnoGene Ltd.). The differentiated chondrogenic cells were fixed for 10 min with 4% paraformaldehyde. Cells were stained with 0.5% Alcian blue in 0.1 N HCl (pH 1.0) overnight, and examined under a light microscope.

Affinity purification

AIMP1 peptide was coupled to Affi-Gel 15 (Bio-Rad) following the manufacturer's instructions. Briefly, Affi-Gel 15 beads were washed thrice with cold deionized water. The beads were incubated with AIMP1 peptide in 10 mM HEPES buffer for 4 h at 4°C. To block non-coupled beads, the beads were further incubated with 1 M ethanolamine-HCl (pH 8.0) for 1 h. The beads were transferred to a column and washed with 10 mM HEPES buffer. To prepare the plasma membrane fraction of BMMSCs, cells were homogenized with 20 strokes of a Dounce homogenizer in Tris-HCl buffer (25 mM Tris-HCl (pH 7.4), 1 mM EDTA, 0.5 mM EGTA, 10 mM NaCl, and protease inhibitor cocktails). One-tenth volume Tris-HCl buffer with 2.5 M sucrose was added to the homogenates. After centrifugation at 1,000*g* for 10 min, the supernatant was carefully harvested and further centrifuged at 15,000*g* for 15 min. The pellet was resuspended in Tris-HCl buffer containing 3 mM $MgCl_2$ and 0.25M sucrose and was designated the plasma membrane fraction. The plasma membrane fraction was then incubated with AIMP1 peptide-coupled bead for 4 h at 4°C and washed thrice with Tris-HCl buffer

containing 3 mM $MgCl_2$ and 0.25M sucrose buffer. The precipitates were then dissolved in SDS sample buffer and subjected to sodium dodecyl sulfate polyacrylamide gel electrophoresis (SDS-PAGE). Bands of interest were in-gel digested with trypsin (Promega). For NanoLC-MS/MS analysis, the peptides were loaded on an Agilent 1100 Series nano-LC and LTQ-mass spectrometer (Thermo Electron). The mobile phase A for LC separation was 0.1% formic acid in deionized water, and the mobile phase B was 0.1% formic acid in acetonitrile. The chromatography gradient was set up to give a linear increase. Mass spectra were acquired using data-dependent acquisition with a full mass scan (400–1800 *m/z*) followed by MS/MS scans. Each MS/MS scan acquired was an average of one microscan on the LTQ. The temperature of the ion transfer tube was maintained at 200°C, and the spray was 1.5.0–2.0 kV. The normalized collision energy was set at 35% for MS/MS. The database search criteria were as follows: taxonomy, *homo sapiens*; fixed modification; carboxyamidomethylated (+57) at cysteine residues; variable modification, oxidized (+16) at methionine residues; maximum allowed missed cleavage, 1; and MS tolerance, 100 ppm. Typical contaminants such as trypsin (used for proteolysis) and keratin were excluded.

Modeling of AIMP1 peptide structure and AIMP1 peptide-FGFR2 docking

The AIMP1 peptide structure was predicted using the Rosetta method that was implemented with the Monte Carlo minimization [28]. The AIMP1 peptide was docked into the binding site of the FGFR2 structure using ClusPro [29–33]. The X-ray structure of FGFR2 (PDB code 1IIL) was used to define the binding site for the molecular docking studies. Energy minimization was conducted for the AIMP1 peptide and FGFR2 with the Amber force field [34] with UCSF Chimera [35]. The standard set parameters were used in all calculations. For energy assessment of the AIMP1 peptide-FGFR2 interaction, FireDock [36,37] with an energy-based score was used. During energy assessment, all values were set to the default values. The APBS program [38] and Coulombic Surface Coloring method with UCSF Chimera were used to calculate the electrostatic surface potentials of the protein-peptide complex model. Electrostatic potential maps were calculated by numerically solving the Poisson–Boltzmann equation based on molecular mechanics. The AIMP1 peptide-FGFR2 complex structure was analyzed and displayed with the UCSF Chimera software [35].

Statistical analysis

SPSS, version 10.0 (SPSS, Inc., Chicago, IL) was used for statistical analysis. The data are expressed as mean ± SD. The differences between the means were calculated using the Mann–Whitney *U*-test. A P-value < 0.05 indicated a statistically significant difference.

Results

AIMP1 peptide induces the phosphorylation of GSK3β, Akt, and ERK via FGFR2 in BMMSCs

In a previous report, we showed that the N-terminus of AIMP1 increased the proliferation of fibroblast via ERK activation to enhance wound repair [20]. To determine whether AIMP1 could activate signaling molecules related to proliferation, a peptide corresponding to the N-terminal residues (amino acids 6–46) of human AIMP1 was added to BMMSCs for various times. AIMP1 induced the phosphorylation of Akt within 5 min, after the phosphorylation of ERK and GSK3β (Fig. 1A). Next, we used affinity purification with the cytoplasmic membrane fraction of BMMSCs to isolate the cognate receptor for AIMP1, as described in the Materials and Methods section. NanoLC-MS/MS analysis showed that AIMP1 peptide bound to FGFR2 (Table 2). We then investigated whether the treatment of AIMP1 peptide to BMMSCs could induce phosphorylation of FGFR2. As shown in Fig. 1B, AIMP1 peptide induced phosphorylation at tyrosine residue of FGFR2. In addition, whether the knock-down of FGFR2 using specific siRNA could abolish the activation of Akt and ERK by AIMP1 peptide was examined. As shown in Fig. 1C, knock-down of FGFR2 abolished Akt and ERK activation by AIMP1 peptide, which suggests that AIMP1 peptide activates Akt and ERK via FGFR2. To predict the potential interaction between AIMP1 peptide and FGFR2, various *in silico* molecular models were generated using the FGFR2 crystal structure previously reported [39], and the best structure was selected based on the energy-based score. In this model, AIMP1 peptide was located on the inner space of FGFR2 that was composed of four subunits, through electrostatic interactions (Supplementary Fig. S1A, B; Supplementary Data are available online at www.liebertpub.com/scd). Negatively charged residues (7Glu, 12Glu, 14Asp, 18Glu, 29Glu, 39Glu, and 40Glu) in AIMP1 peptide were predicted to contribute to the interaction with positively charged residues in FGFR2 (Supplementary Fig. S1C). In addition, hydrogen bonds between AIMP1 peptide and FGFR2 stabilized the complex structure. In this model, five hydrogen bonds involving four residues of AIMP1 peptide residues (9Lys, 12Glu, 25Ser, and 28Lys), were found at the binding interface, which suggested an extensive interaction between AIMP1 peptide and FGFR2 (Supplementary Fig. S1C). In addition, the energy-based score of the complex was −160.93 from the FireDock results (Supplementary Fig. S1D)

GSK3β is a cytoplasmic serine/threonine kinase that regulates Wnt/β-catenin, Hedgehog, Notch, and insulin signaling [40]. Moreover, the phosphorylation of Ser9 in GSK3β by phosphorylated Akt decreases the activity of GSK3β [41]. Therefore, the relationship between the phosphorylation of GSK3β and Akt activation was examined. Pretreatment with LY294002, a PI3K inhibitor, abolished the phosphorylation of Akt and GSK3β; whereas pre-treatment with U1026, an ERK inhibitor, did not eliminate the phosphorylation of Akt and GSK3β. These findings suggest that activation of Akt by AIMP1 peptide is prerequisite for the phosphorylation of GSK3β (Fig. 1D).

AIMP1 peptide enhances the protein stability and nuclear translocation of β-catenin

GSK3β phosphorylates β-catenin in the Wnt/β-catenin signaling pathway, leading to the ubiquitination and proteasomal-dependent degradation of β-catenin [42]. Since the phosphorylation of GSK3β by Akt activation prevents the proteasomal degradation of β-catenin, we evaluated whether AIMP1 peptide could induce the accumulation of non-phosphorylated β-catenin via Akt in BMMSCs. Immunoblot analysis clearly showed that AIMP1 increased the β-catenin

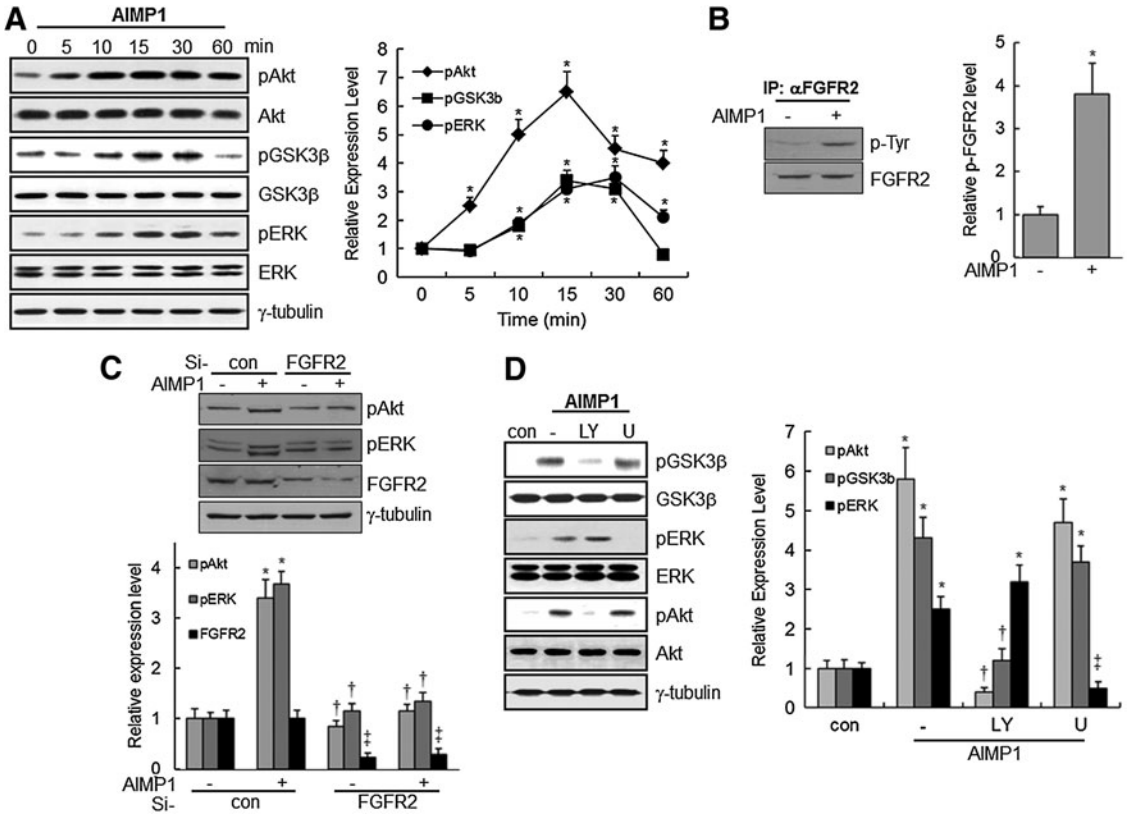

FIG. 1. ARS-Interacting Multi-functional Protein 1 (AIMP1) induces the phosphorylation of Akt, ERK, and glycogen synthase kinase-3β (GSK3β) via fibroblast growth factor receptor 2 (FGFR2) in human bone marrow-derived mesenchymal stem cells (BMMSCs). **(A)** AIMP1 peptide (100 ng/mL) was added to BMMSCs for the indicated time. Cell extracts were harvested and blotted with specific antibodies. In densitometric analysis, the intensity of phosphorylated protein was normalized to that of total protein. *, vs. time 0. **(B)** AIMP1 peptide (100 ng/mL) was added to BMMSCs for 5 min. Immunoprecipitation using anti-FGFR2 antibody was performed. Phosphorylation level of FGFR2 was detected with p-Tyr antibody (Santa Cruz Biotechnology). In densitometric analysis, the intensity of p-Tyr protein was normalized to that of immunoprecipitated protein. *, vs. AIMP1-. **(C)** Control si-RNA or FGFR2 si-RNA (Santa Cruz Biotechnology) was transfected into BMMSCs using Lipofectamine 2000 for 48 h. Cells were then starved for 12 h, and AIMP1 peptide was added to BMMSCs for 15 min. Cell extracts were harvested and blotted with specific antibodies. For densitometric analysis, the intensity of phosphorylated protein was normalized to that of tubulin band (*, vs. AIMP1-/Si-con; †, vs. AIMP + /Si-con; ‡, vs. Si-con). **(D)** BMMSCs were treated with 10 μM of LY294002 and U1026 for 5 min and with AIMP1 peptide (100 ng/mL) for 15 min. Protein extracts were harvested and blotted with specific antibodies. Tubulin was used as a loading control. For densitometric analysis, the intensity of phosphorylated protein was normalized to that of total protein (*, vs. control; †, vs. AIMP1 alone; ‡, vs. AIMP1 alone and LY + AIMP1). Data are the means of at least three independent experiments. Values are the mean ± SD. $^{*}P < 0.01$, $^{\dagger}P < 0.01$, $^{\ddagger}P < 0.01$.

level in a dose-dependent manner; treatment with LY294002 abolished this increase (Fig. 2A, B). In addition, we examined whether β-catenin translocated into the nucleus in response to AIMP1. Protein extracts were fractionated into cytoplasmic and nuclear fractions, and β-catenin was detected with a specific antibody. As shown in Fig. 2C, β-catenin accumulated in the nucleus after treatment with AIMP1 peptide. Furthermore, immunofluorescence staining of β-catenin clearly showed that AIMP1 peptide induced the translocation of β-catenin into the nucleus (Fig. 2D). Pretreatment with LY294002, but not U0126, inhibited the nuclear accumulation of β-catenin by AIMP1, further confirming that the nuclear

Table 2. Protein Identities Determined by LC-MS/MS

Accession number	*Protein name*	*Score*[a]	*Matched peptides number*	*Sequence coverage (%)*	*Matching sequence*	*Theoretical MW/pI*
gi|4883533	Fibroblast growth receptor 2 IgIIIb isoform	70	5	13.7	YGPDGLPYLKVLK RQVSAESSSSMNSNTPLVR EAVGIDKDKPK DDATEKDLSDLVSEMEMMKMIGK TTNGRLPVK	65417/6.28

[a]Score is $-10 \times \mathrm{Log}(P)$, where P is the probability that the observed match is a random event; it is based on NCBInr database using the MASCOT searching program as LC-MS data.

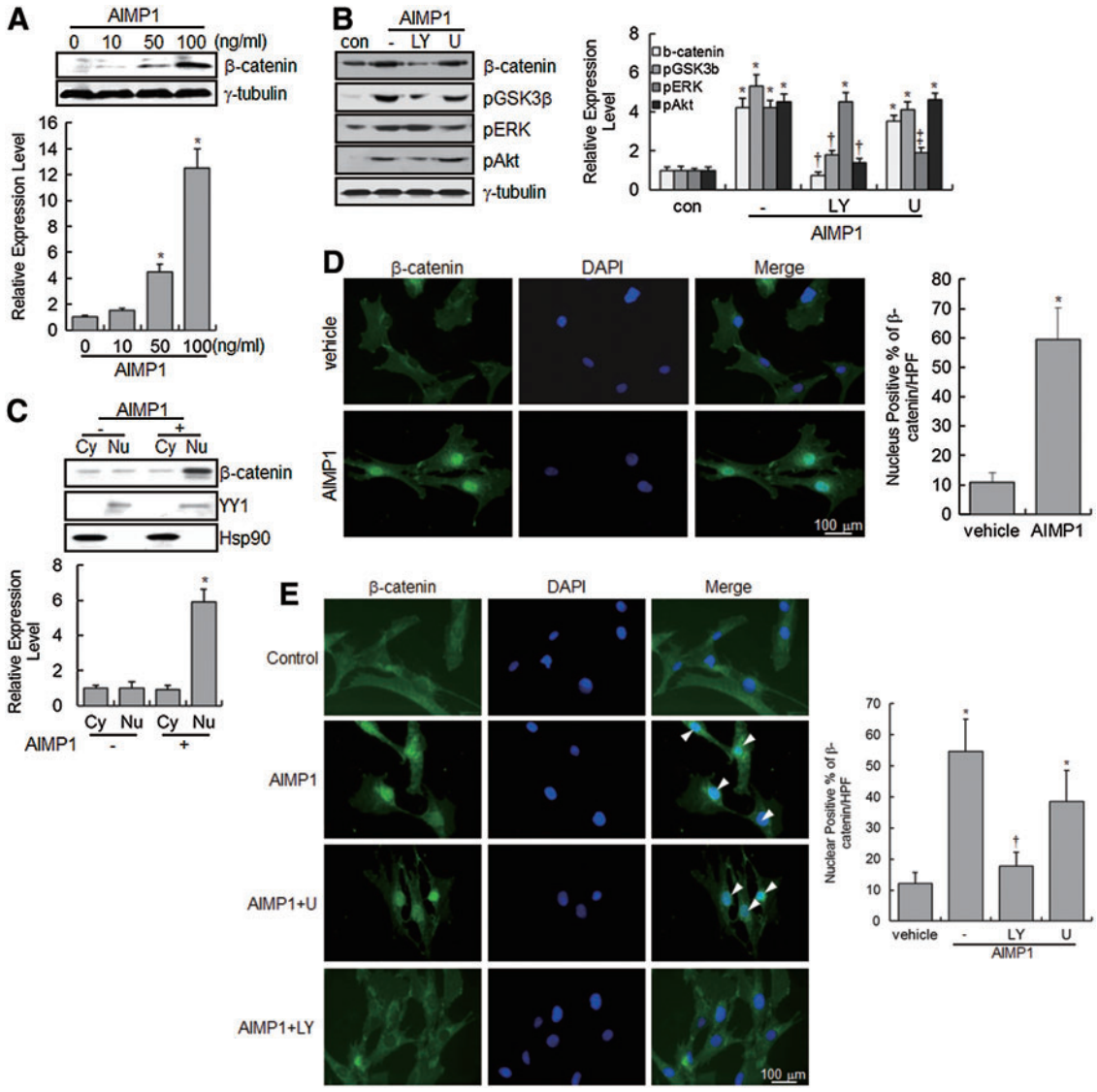

FIG. 2. AIMP1 induces the stabilization and nuclear translocation of β-catenin in human BMMSCs. **(A)** BMMSCs were treated with different concentrations of AIMP1 peptide for 2 h. Protein extracts were harvested and blotted with the indicated antibodies. The densitometric analysis from western blotting is shown. The β-catenin level was normalized to the tubulin level. *, vs. time 0. **(B)** BMMSCs were treated with LY294002 (10 μM) and U1026 (10 μM) for 5 min and with AIMP1 peptide (100 ng/mL) for 15 min. Protein extracts were subjected to sodium dodecyl sulfate polyacrylamide gel electrophoresis and blotted with the indicated antibodies. Tubulin was used as a loading control. For densitometric analysis, the intensity of each band was normalized to that of the corresponding tubulin band (*, vs. control; †, vs. AIMP1 alone; ‡, vs. AIMP1 alone and LY + AIMP1). **(C)** After treatment of BMMSCs with AIMP1 (100 ng/mL) for 2 h, cells were fractionated into cytoplasmic and nuclear fractions, and protein extracts were blotted with β-catenin antibody. Yin Yang 1(YY1) and heat shock protein 90 (HSP90) were used as nuclear and cytoplasmic markers, respectively. Cytoplasmic β-catenin was normalized to Hsp90, and nuclear β-catenin was normalized to YY1 (*, vs. nuclear fraction of AIMP1 negative). **(D, E)** BMMSCs were treated with AIMP1 peptide (100 ng/mL), and immunofluorescence staining was performed as described in the Materials and Methods section. β-catenin (*green*) was stained with FITC-conjugated anti-mouse antibody. The nuclei (*blue*) were counterstained with diamidino-2-phenylindole. The number of nuclear β-catenin positive cells was counted in at least four different fields under high power (20X) (*, vs. vehicle; †, vs. AIMP1 alone). Data are the means of at least three independent experiments. Values are the mean ± SD. $^{*}P < 0.01$, $^{\dagger}P < 0.01$, $^{\ddagger}P < 0.01$. Color images available online at www.liebertpub.com/scd

translocation of β-catenin induced by AIMP1 peptide was mediated by the activation of Akt (Fig. 2E).

AIMP1 peptide increases cyclin D1 and c-myc expression via the β-catenin/TCF complex

Nuclear accumulation of β-catenin stimulates the activation of the lymphoid-enhancer factor (LEF)/TCF complex, leading to the transcriptional up-regulation of downstream target genes, including cyclin D1 and c-myc, which are critical for cell proliferation and development [43,44]. We investigated whether the nuclear accumulation of β-catenin, induced by AIMP1 peptide, activated the LEF/TCF complex. First, a luciferase assay was performed using a TOPflash vector with LEF/TCF-binding sites. AIMP1 peptide significantly increased the luciferase activity about four-fold

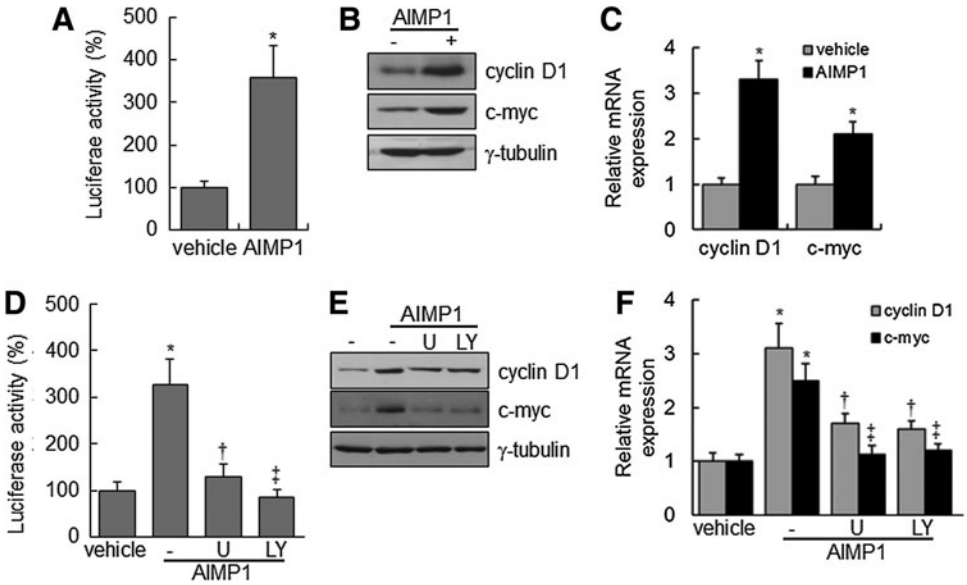

FIG. 3. AIMP1 increases the transcriptional activity of T-cell factor (TCF) in human BMMSCs. BMMSCs expressing TOPflash vector were treated with AIMP1 peptide (100 ng/mL) and harvested. **(A)** Luciferase activity was measured. **(B, C)** The expression of cyclin D1 and c-myc was examined by immunoblot and quantitative reverse transcription-polymerase chain reaction (PCR) analysis, respectively. **(D)** The transcriptional activity of TCF was examined in the presence or absence of U0126 (10 μM) or LY294002 (10 μM). (†, vs. AIMP1 alone; ‡, vs. AIMP1 alone). **(E, F)** In addition, the expression of TCF target genes was examined by immunoblot and qRT-PCR analysis, respectively. (†, vs. cyclin D1 of AIMP1 alone; ‡, vs. c-myc of AIMP1 alone). Data represent the mean ± SD of three independent experiments. $^{*}P < 0.01$, $^{\dagger}P < 0.05$, $^{\ddagger}P < 0.01$.

compared with the control treatment (Fig. 3A). Western blot and qRT-PCR analyses showed that AIMP1 peptide increased the expression of cyclin D1 and c-myc at the transcriptional level (Fig. 3B, C). In addition, the correlation between the activation of Akt, ERK, and the LEF/TCF complex was investigated. Pre-treatment with U1026 and LY294002 suppressed the increase in luciferase activity induced by AIMP1 peptide. These results suggested that the activation of Akt and ERK by AIMP1 peptide was critical to the increased activity of the LEF/TCF complex (Fig. 3D). Western blot and qRT-PCR analyses supported that the increase in cyclin D1 and c-myc expression induced by AIMP1 peptide was regulated at the transcriptional level via Akt and ERK activation (Fig. 3E, F). We knocked down β-catenin using specific si-RNA and examined whether the increases in luciferase activity and in cyclin D1 and c-myc expression are mediated via the stabilization of β-catenin induced by AIMP1 peptide. As shown in Fig. 4A, knock-down of β-catenin abrogated the increase in luciferase activity induced by AIMP1 peptide. Western blot and qRT-PCR analyses showed that the increase in cyclin D1 and c-myc expression induced by AIMP1 peptide is mediated by β-catenin (Fig. 4B, C). In addition, DN TCF inhibited the increase in TOPflash luciferase activity induced by AIMP1 peptide in a dose-dependent manner (Fig. 4D). Western blot and qRT-PCR analyses further supported that the activation of the LEF/TCF complex by AIMP1 peptide played a critical role in increasing the expression of cyclin D1 and c-myc (Fig. 4E, F).

AIMP1 increases the proliferation of human BMMSCs

The induction of cyclin D1 and c-myc genes by the activation of the LEF/TCF complex is critical for cell cycle progression [43,45]. Therefore, we investigated whether the increase in cyclin D1 and c-myc expression induced by AIMP1 peptide could lead to promoting the proliferation of BMMSCs. First, AIMP1 peptide was treated to MSCs for 24 h, and the MTT assay was performed. AIMP1 peptide stimulated the proliferation of BMMSCs in a dose-dependent manner (Fig. 5A). In addition, the proliferation-inducing activity of AIMP1 peptide was examined to determine whether it could lead to an increase in the number of cells. AIMP1 peptide was added to BMMSCs in a time-dependent manner, and the number of cells was counted at the times indicated. AIMP1 peptide significantly increased the proliferation of BMMSCs in a time-dependent manner compared with control treatments (Fig. 5B). The knock-down of β-catenin using specific si-RNA inhibited the proliferation of BMMSCs induced by AIMP1 peptide in both the MTT assay and the cell counting assays (Fig. 5C, D). DN TCF also suppressed the proliferation of BMMSCs induced by AIMP1 peptide, further confirming that AIMP1 peptide induced the proliferation of BMMSCs through the LEF/TCF complex via the stabilization of β-catenin (Fig. 5E, F). We further examined whether AIMP1 peptide would affect the differentiation of human BMMSCs into adipocytes, chondrocytes, and osteoblasts. However, the differentiation of BMMSCs into each phenotype was not affected by treatment with AIMP1 peptide (data not shown).

AIMP1 peptide increases colony formation of MSCs

We injected AIMP1 peptide into the intraperitonium of mouse and analyzed colony-forming ability using mononuclear cells isolated from peripheral blood. AIMP1 peptide significantly increased fibroblast-like colony formation in a

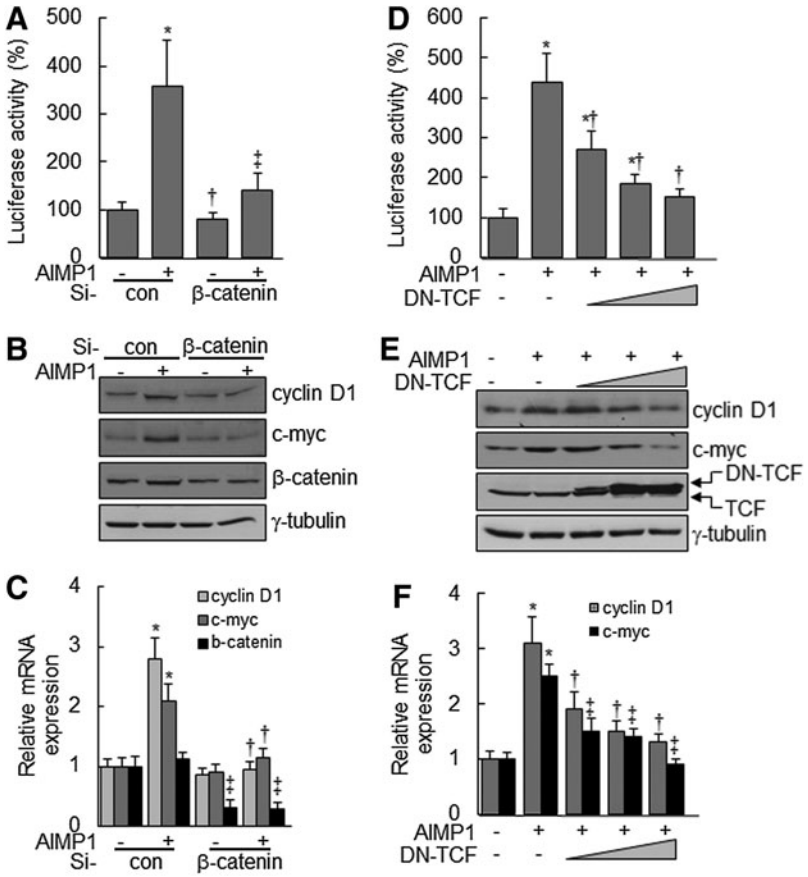

FIG. 4. AIMP1 increases the expression of cyclin D1 and c-myc via β-catenin and TCF. **(A–C)** β-catenin-specific si-RNA mixture (20 nM) covering different three sequences or control si-RNA (Santa Cruz Biotechnology) was transfected into BMMSCs for 24 h. The TOPflash vector and the *Renilla* luciferase vector were then transfected for 12 h. After serum starvation for 12 h, cells were treated with AIMP1 peptide (100 ng/mL) for 24 h. Cells were harvested for luciferase activity analysis. The expression of cyclin D1 and c-myc was examined by immunoblot and qRT-PCR analysis. **(D–F)** TOPflash, *Renilla* luciferase, and dominant negative (DN) TCF vectors were transfected into BMMSCs for 12 h. After serum starvation for 12 h, cells were treated with AIMP1 peptide (100 ng/mL) for 24 h. The luciferase activity was analyzed. Target gene expression was assessed by immunoblot and qRT-PCR. Data represent the mean ± SD of three independent experiments. $^*P < 0.01$.

dose- and time-dependent manner (Fig. 6A, B). To determine whether the fibroblast-like cells were MSCs, flow cytometry was performed using a variety of MSC markers. The cultured fibroblast-like cells were positive for CD105, CD44, CD90, and CD29, but negative for CD34 and CD45, which is characteristic of MSCs (Fig. 6C). Therefore, we next examined whether the isolated fibroblast-like cells could differentiate into other cells such as adipocytes, osteocytes, and chondrocytes. As shown in Fig. 6D, fibroblast-like cells efficiently differentiated into adipocytes, osteocytes, and

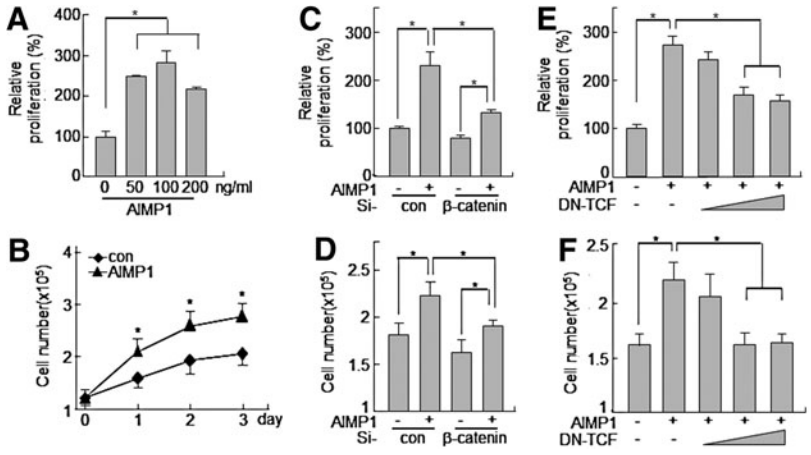

FIG. 5. AIMP1 peptide enhances the proliferation of human BMMSCs. **(A)** Human BMMSCs were treated with the indicated concentration of AIMP1 for 24 h, and cell proliferation was analyzed by WST1 assay. **(B)** Human BMMSCs (1×10^5 cells) were seeded onto six-well plates and cultured for 24 h. AIMP1 peptide (100 ng/mL) was added every 24 h, and the cell number was counted. **(C, D)** After transfection with control si-RNA or β-catenin si-RNA (20 nM) to human BMMSCs for 24 h, human BMMSCs were treated with AIMP1 peptide (100 ng/mL) for 24 h. Cell proliferation was examined by the WST1 assay and cell counting. **(E, F)** After transfection with DN-TCF for 12 h, human BMMSCs were treated with AIMP1 peptide (100 ng/mL) for 24 h. Cell proliferation was examined by the WST1 assay and cell counting. Data represent the mean ± SD of three independent experiments. $^*P < 0.01$.

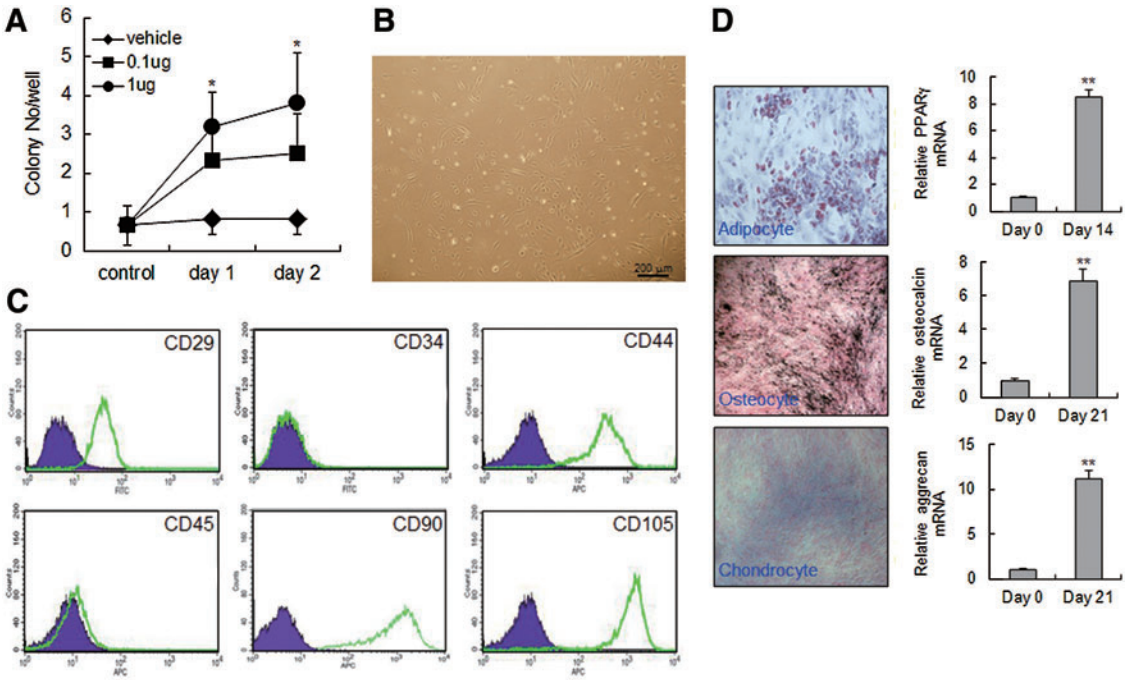

FIG. 6. AIMP1 peptide stimulates colony formation of mouse MSCs. **(A, B)** C57/BL6 mice ($n=10$ per group) were intraperitoneally injected with different doses of AIMP1 peptide. Mononuclear cells were harvested from peripheral blood at different times and seeded onto gelatin-coated wells as described in the Materials and Methods section. After 2 weeks, the number of colonies was counted. **(C)** Flow cytometry analysis was performed using colony-forming cells (passage 3). Cells were labeled with the indicated fluorescent-conjugated antibodies, and cells were analyzed with an FACScalibur flow cytometer. The *purple area* indicates the negative control, and the *green line* represents specific staining with the indicated antibodies. A representative image from three individual experiments is shown. **(D)** *Left*: The colony-forming cells were subjected to differentiation into adipocytes, osteocytes, and chondrocytes as described in the Materials and Methods section. *Right*—qRT-PCR was performed using cDNA isolated from control or differentiated cells. Data are the means of at least three independent experiments. Data represent the mean ± SD. $^{*}P<0.05$, $^{**}P<0.01$. Color images available online at www.liebertpub.com/scd

chondrocytes, confirming that the colonies of fibroblast-like cells induced by AIMP1 peptide were MSCs.

Discussion

BMMSCs have been studied as a potential source of material for cell therapy. However, it is difficult to obtain an adequate supply of MSCs from a single patient. Moreover, methods for the ex vivo manipulation of MSCs are poorly developed due to the animal source for cell manipulation. Thus, the development of an in vitro expansion method that preserves the differentiation and proliferative potential of MSCs has been suggested. Recently, S1P, EGF, and FGF were shown to induce the proliferation of MSCs without affecting their multipotency [14–17]. In our previous report, we suggested that AIMP1 could function as a growth factor to induce fibroblast proliferation [20]. Therefore, we examined whether AIMP1 peptide could induce the proliferation of MSCs. First, the ability of AIMP1 peptide to activate the signaling mediators, including Akt, ERK, JNK, and p38 MAPK, was examined. AIMP1 was previously shown to activate a variety of signaling molecules in various cell lines [20,23,25,46]. Consistently, in our study, AIMP1 peptide activated Akt in BMMSCs, leading to the inhibition of GSK3β. Since GSK3β plays a critical role in the regulation of β-catenin stability when Wnt is stimulated, we investigated whether AIMP1 peptide, similar to Wnt, could inhibit GSK3β via the activation of APC complex. However, AIMP1 peptide did not induce the phosphorylation of disheveled (Dvl) or the interaction of axin with low-density lipoprotein receptor-related protein 5/6, indicating that AIMP1 peptide did not activate the canonical Wnt signaling pathway (data not shown). In addition, inhibition of Akt using LY294002 abolished the accumulation and the nuclear translocation of β-catenin after stimulation with AIMP1 peptide. This suggests that AIMP1 peptide promoted the stabilization of β-catenin via the activation of Akt in a Wnt-independent manner.

In this study, AIMP1 peptide was shown to activate ERK (Fig. 1); treatment with U0126 inhibited the phosphorylation of ERK but not Akt. In addition, the inhibition of Akt activity using LY294002 did not suppress ERK phosphorylation. The findings suggest that AIMP1 peptide induced the phosphorylation of ERK independent of Akt activation: AIMP1 activated Akt and ERK via FGFR2 as shown in Fig. 1B, and Supplementary Fig. S1. FGFR downstream signaling occurs through two main pathways: the Ras-dependent MAPK pathway and the Ras-independent PI3K-Akt pathway [47,48]. Interestingly, inhibition of ERK phosphorylation suppressed the expression of LEF/TCF target genes induced by AIMP1 peptide (Fig. 3D); whereas AIMP1 peptide-induced β-catenin accumulation and nuclear translocation were not affected (Fig. 2B). Considering that phosphorylated ERK accumulates in the nucleus and activates TCF/Elk-1 for the expression of downstream target genes [49–51], it appears that AIMP1

peptide increased the proliferation of BMMSCs by inducing the expression of TCF target genes via the activation of ERK as well as Akt via FGFR. In addition, the down-regulation of β-catenin using si-RNA and DN TCF abrogated the increase in cell proliferation induced by AIMP1 peptide, further supporting the fact that AIMP1 peptide induced cell proliferation via sequential stimulation of β-catenin and the TCF complex through the activation of Akt and ERK.

AIMP1 peptide stimulated the colony-forming ability of MSCs in peripheral blood, indicating that AIMP peptide increased the population of MSC precursor cells. However, it is not clear whether the increased population of peripheral blood MSCs induced by AIMP1 peptide was a result of increased proliferation in peripheral blood or mobilization from BM. Further studies are required to unveil the exact mechanism. Taken together, the results of this study suggest that AIMP1 peptide induces the expression of cyclin D1 and c-myc by activating the β-catenin/TCF complex through activation of ERK and Akt via FGFR2, leading to the proliferation of BMMSCs. Since AIMP1 peptide has FGF-like activity in promoting the proliferation of MSCs, AIMP1 peptide might be a useful tool with which to manipulate MSCs in vitro.

Acknowledgments

This research was supported by the Bio & Medical Technology Development Program of the National Research Foundation (NRF) funded by the Korean government (MEST) (2012M3A9C6049719).

Author Disclosure Statement

The authors declare no competing financial interests.

References

1. Cho KJ, KA Trzaska, SJ Greco, J McArdle, FS Wang, JH Ye and P Rameshwar. (2005). Neurons derived from human mesenchymal stem cells show synaptic transmission and can be induced to produce the neurotransmitter substance P by interleukin-1 alpha. Stem Cells 23:383–391.
2. Rose RA, H Jiang, X Wang, S Helke, JN Tsoporis, N Gong, SC Keating, TG Parker, PH Backx and A Keating. (2008). Bone marrow-derived mesenchymal stromal cells express cardiac-specific markers, retain the stromal phenotype, and do not become functional cardiomyocytes in vitro. Stem Cells 26:2884–2892.
3. Schulze M, F Belema-Bedada, A Technau and T Braun. (2005). Mesenchymal stem cells are recruited to striated muscle by NFAT/IL-4-mediated cell fusion. Genes Dev 19:1787–1798.
4. Snykers S, J De Kock, V Rogiers and T Vanhaecke. (2009). In vitro differentiation of embryonic and adult stem cells into hepatocytes: state of the art. Stem Cells 27:577–605.
5. Oswald J, S Boxberger, B Jorgensen, S Feldmann, G Ehninger, M Bornhauser and C Werner. (2004). Mesenchymal stem cells can be differentiated into endothelial cells in vitro. Stem Cells 22:377–384.
6. Jiang Y, BN Jahagirdar, RL Reinhardt, RE Schwartz, CD Keene, XR Ortiz-Gonzalez, M Reyes, T Lenvik, T Lund, et al. (2002). Pluripotency of mesenchymal stem cells derived from adult marrow. Nature 418:41–49.
7. Pereira RF, KW Halford, MD O'Hara, DB Leeper, BP Sokolov, MD Pollard, O Bagasra and DJ Prockop. (1995). Cultured adherent cells from marrow can serve as long-lasting precursor cells for bone, cartilage, and lung in irradiated mice. Proc Natl Acad Sci U S A 92:4857–4861.
8. Friedenstein AJ, JF Gorskaja and NN Kulagina. (1976). Fibroblast precursors in normal and irradiated mouse hematopoietic organs. Exp Hematol 4:267–274.
9. Wagner W, F Wein, A Seckinger, M Frankhauser, U Wirkner, U Krause, J Blake, C Schwager, V Eckstein, W Ansorge and AD Ho. (2005). Comparative characteristics of mesenchymal stem cells from human bone marrow, adipose tissue, and umbilical cord blood. Exp Hematol 33:1402–1416.
10. Katz AJ, A Tholpady, SS Tholpady, H Shang and RC Ogle. (2005). Cell surface and transcriptional characterization of human adipose-derived adherent stromal (hADAS) cells. Stem Cells 23:412–423.
11. Kern S, H Eichler, J Stoeve, H Kluter and K Bieback. (2006). Comparative analysis of mesenchymal stem cells from bone marrow, umbilical cord blood, or adipose tissue. Stem Cells 24:1294–1301.
12. Dominici M, K Le Blanc, I Mueller, I Slaper-Cortenbach, F Marini, D Krause, R Deans, A Keating, D Prockop and E Horwitz. (2006). Minimal criteria for defining multipotent mesenchymal stromal cells. The International Society for Cellular Therapy position statement. Cytotherapy 8:315–317.
13. Pittenger MF, AM Mackay, SC Beck, RK Jaiswal, R Douglas, JD Mosca, MA Moorman, DW Simonetti, S Craig and DR Marshak. (1999). Multilineage potential of adult human mesenchymal stem cells. Science 284:143–147.
14. Tamama K, VH Fan, LG Griffith, HC Blair and A Wells. (2006). Epidermal growth factor as a candidate for *ex vivo* expansion of bone marrow-derived mesenchymal stem cells. Stem Cells 24:686–695.
15. Choi SC, SJ Kim, JH Choi, CY Park, WJ Shim and DS Lim. (2008). Fibroblast growth factor-2 and -4 promote the proliferation of bone marrow mesenchymal stem cells by the activation of the PI3K-Akt and ERK1/2 signaling pathways. Stem Cells Dev 17:725–736.
16. Calarco A, O Petillo, M Bosetti, A Torpedine, M Cannas, L Perrone, U Galderisi, MA Melone and G Peluso. (2010). Controlled delivery of the heparan sulfate/FGF-2 complex by a polyelectrolyte scaffold promotes maximal hMSC proliferation and differentiation. J Cell Biochem 110:903–909.
17. He X, C H'Ng S, DT Leong, DW Hutmacher and AJ Melendez. (2010). Sphingosine-1-phosphate mediates proliferation maintaining the multipotency of human adult bone marrow and adipose tissue-derived stem cells. J Mol Cell Biol 2:199–208.
18. Quevillon S, F Agou, JC Robinson and M Mirande. (1997). The p43 component of the mammalian multi-synthetase complex is likely to be the precursor of the endothelial monocyte-activating polypeptide II cytokine. J Biol Chem 272:32573–32579.
19. Matschurat S, UE Knies, V Person, L Fink, B Stoelcker, C Ebenebe, HA Behrensdorf, J Schaper and M Clauss. (2003). Regulation of EMAP II by hypoxia. Am J Pathol 162:93–103.
20. Park SG, H Shin, YK Shin, Y Lee, EC Choi, BJ Park and S Kim. (2005). The novel cytokine p43 stimulates dermal fibroblast proliferation and wound repair. Am J Pathol 166:387–398.
21. Kim E, SH Kim, S Kim, D Cho and TS Kim. (2008). AIMP1/p43 protein induces the maturation of bone marrow-derived dendritic cells with T helper type 1-polarizing ability. J Immunol 180:2894–2902.
22. Kim E, SH Kim, S Kim and TS Kim. (2006). The novel cytokine p43 induces IL-12 production in macrophages via NF-

kappaB activation, leading to enhanced IFN-gamma production in CD4+ T cells. J Immunol 176:256–264.
23. Ko Y-G, H Park, T Kim, J-W Lee, SG Park, W Seol, JE Kim, W-H Lee, S-H Kim, JE Park and S Kim. (2001). A cofactor of tRNA synthetase, p43, is secreted to up-regulate proinflammatory genes. J Biol Chem 276:23028–32303.
24. Park H, SG Park, J-W Lee, T Kim, G Kim, Y-G Ko and S Kim. (2002). Monocyte cell adhesion induced by a human aminoacyl-tRNA synthetase associated factor, p43: identification of the related adhesion molecules and signal pathways. J Leukoc Biol 71:223–230.
25. Park SG, YS Kang, YH Ahn, SH Lee, KR Kim, KW Kim, GY Koh, YG Ko and S Kim. (2002). Dose-dependent biphasic activity of tRNA synthetase-associating factor, p43, in angiogenesis. J Biol Chem 277:45243–45248.
26. Park SG, YS Kang, JY Kim, CS Lee, YG Ko, WJ Lee, KU Lee, YI Yeom and S Kim. (2006). Hormonal activity of AIMP1/p43 for glucose homeostasis. Proc Natl Acad Sci U S A 103:14913–14918.
27. Han JM, SG Park, Y Lee and S Kim. (2006). Structural separation of different extracellular activities in aminoacyl-tRNA synthetase-interacting multi-functional protein, p43/AIMP1. Biochem Biophys Res Commun 342:113–118.
28. Leaver-Fay A, M Tyka, SM Lewis, OF Lange, J Thompson, R Jacak, K Kaufman, PD Renfrew, CA Smith, et al. (2011). ROSETTA3: an object-oriented software suite for the simulation and design of macromolecules. Methods Enzymol 487:545–574.
29. Kozakov D, DR Hall, D Beglov, R Brenke, SR Comeau, Y Shen, K Li, J Zheng, P Vakili, I Paschalidis and S Vajda. (2010). Achieving reliability and high accuracy in automated protein docking: ClusPro, PIPER, SDU, and stability analysis in CAPRI rounds 13–19. Proteins 78:3124–3130.
30. Kozakov D, R Brenke, SR Comeau and S Vajda. (2006). PIPER: an FFT-based protein docking program with pairwise potentials. Proteins 65:392–406.
31. Comeau SR, DW Gatchell, S Vajda and CJ Camacho. (2004). ClusPro: a fully automated algorithm for protein-protein docking. Nucleic Acids Res 32:W96–W99.
32. Comeau SR, DW Gatchell, S Vajda and CJ Camacho. (2004). ClusPro: an automated docking and discrimination method for the prediction of protein complexes. Bioinformatics 20:45–50.
33. Benyamini H and A Friedler. (2011). The ASPP interaction network: electrostatic differentiation between pro- and anti-apoptotic proteins. J Mol Recognit 24:266–274.
34. Case DA, TE Cheatham, 3rd., T Darden, H Gohlke, R Luo, KM Merz, Jr., A Onufriev, C Simmerling, B Wang and RJ Woods. (2005). The Amber biomolecular simulation programs. J Comput Chem 26:1668–1688.
35. Pettersen EF, TD Goddard, CC Huang, GS Couch, DM Greenblatt, EC Meng and TE Ferrin. (2004). UCSF Chimera—a visualization system for exploratory research and analysis. J Comput Chem 25:1605–1612.
36. Andrusier N, R Nussinov and HJ Wolfson. (2007). FireDock: fast interaction refinement in molecular docking. Proteins 69:139–159.
37. Mashiach E, D Schneidman-Duhovny, N Andrusier, R Nussinov and HJ Wolfson. (2008). FireDock: a web server for fast interaction refinement in molecular docking. Nucleic Acids Res 36:W229–W232.
38. Baker NA, D Sept, S Joseph, MJ Holst and JA McCammon. (2001). Electrostatics of nanosystems: application to microtubules and the ribosome. Proc Natl Acad Sci U S A 98:10037–10041.
39. Ibrahimi OA, AV Eliseenkova, AN Plotnikov, K Yu, DM Ornitz and M Mohammadi. (2001). Structural basis for fibroblast growth factor receptor 2 activation in Apert syndrome. Proc Natl Acad Sci U S A 98:7182–7187.
40. Cohen P and S Frame. (2001). The renaissance of GSK3. Nat Rev Mol Cell Biol 2:769–776.
41. Cross DA, DR Alessi, P Cohen, M Andjelkovich and BA Hemmings. (1995). Inhibition of glycogen synthase kinase-3 by insulin mediated by protein kinase B. Nature 378:785–789.
42. Liu C, Y Li, M Semenov, C Han, GH Baeg, Y Tan, Z Zhang, X Lin and X He. (2002). Control of beta-catenin phosphorylation/degradation by a dual-kinase mechanism. Cell 108:837–847.
43. Behrens J, JP von Kries, M Kuhl, L Bruhn, D Wedlich, R Grosschedl and W Birchmeier. (1996). Functional interaction of beta-catenin with the transcription factor LEF-1. Nature 382:638–642.
44. Molenaar M, M van de Wetering, M Oosterwegel, J Peterson-Maduro, S Godsave, V Korinek, J Roose, O Destree and H Clevers. (1996). XTcf-3 transcription factor mediates beta-catenin-induced axis formation in Xenopus embryos. Cell 86:391–399.
45. Willert K and KA Jones. (2006). Wnt signaling: is the party in the nucleus? Genes Dev 20:1394–1404.
46. Park H, SG Park, J Kim, YG Ko and S Kim. (2002). Signaling pathways for TNF production induced by human aminoacyl-tRNA synthetase-associating factor, p43. Cytokine 20:148–153.
47. Brooks AN, E Kilgour and PD Smith. (2012). Molecular pathways: fibroblast growth factor signaling: a new therapeutic opportunity in cancer. Clin Cancer Res 18:1855–1862.
48. Coutu DL and J Galipeau. (2011). Roles of FGF signaling in stem cell self-renewal, senescence and aging. Aging (Albany NY) 3:920–933.
49. Gille H, M Kortenjann, O Thomae, C Moomaw, C Slaughter, MH Cobb and PE Shaw. (1995). ERK phosphorylation potentiates Elk-1-mediated ternary complex formation and transactivation. EMBO J 14:951–962.
50. Gille H, AD Sharrocks and PE Shaw. (1992). Phosphorylation of transcription factor p62TCF by MAP kinase stimulates ternary complex formation at c-fos promoter. Nature 358:414–417.
51. Marais R, J Wynne and R Treisman. (1993). The SRF accessory protein Elk-1 contains a growth factor-regulated transcriptional activation domain. Cell 73:381–393.

Address correspondence to:
Prof. Sang Gyu Park
Laboratory for Tracing of Gene Function
Department of Biomedical Science
CHA University
502, Yatap-dong, Bundang-gu
Sungnam-si, Gyeonggi-do 463-80
Korea

E-mail: sgpark@cha.ac.kr

Received for publication December 23, 2012
Accepted after revision May 13, 2013
Prepublished on Liebert Instant Online May 14, 2013